Neuron, Vol. 46, 773–785, June 2, 2005, Copyright ©2005 by Elsevier Inc. DOI 10.1016/j.neuron.2005.04.025

Climbing Fiber Innervation of NG2-Expressing Glia in the Mammalian Cerebellum

Shih-chun Lin,[1] Jojanneke H.J. Huck,[2] J. David B. Roberts,[2] Wendy B. Macklin,[3] Peter Somogyi,[2] and Dwight E. Bergles[1,*]
[1]Department of Neuroscience
Johns Hopkins University School of Medicine
Baltimore, Maryland 21205
[2]Medical Research Council
Anatomical Neuropharmacology Unit
Mansfield Road
Oxford, OX1 3TH
United Kingdom
[3]Department of Neurosciences
Lerner Research Institute
Cleveland Clinic Foundation
Cleveland, Ohio 44195

Summary

The molecular layer of the cerebellar cortex is populated by glial progenitors that express ionotropic glutamate receptors and extend numerous processes among Purkinje cell dendrites. Here, we show that release of glutamate from climbing fiber (CF) axons produces AMPA receptor currents with rapid kinetics in these NG2-immunoreactive glial cells (NG2$^+$ cells) in cerebellar slices. NG2$^+$ cells may receive up to 70 discrete inputs from one CF and, unlike mature Purkinje cells, are often innervated by multiple CFs. Paired Purkinje cell-NG2$^+$ cell recordings show that one CF can innervate both cell types. CF boutons make direct synaptic junctions with NG2$^+$ cell processes, indicating that this rapid neuron-glia signaling occurs at discrete sites rather than through ectopic release at CF-Purkinje cell synapses. This robust activation of Ca^{2+}-permeable AMPA receptors in NG2$^+$ cells expands the influence of the olivocerebellar projection to this abundant class of glial progenitors.

Introduction

Climbing fibers (CFs) from the inferior olive provide a major glutamatergic projection to the cerebellum that helps to maintain equilibrium, relay movement errors, and enable plasticity in motor output (Ohyama et al., 2003). The powerful excitation of Purkinje cells (PCs) by these axons is central to their ability to exert control over motor systems; it drives inhibition of output neurons in the deep cerebellar nuclei and allows heterosynaptic modulation of other inputs to PCs, including long-term depression of parallel fiber (PF)-PC synapses (Ito and Kano, 1982) and changes in the strength of inhibitory synapses (Kano et al., 1992). Whether all aspects of CF control can be attributed to the innervation of PCs remains controversial. Physiological studies suggest that some cerebellar interneurons may receive weak monosynaptic input from CFs (Eccles et al., 1966; Jorntell and Ekerot, 2003), although defined synaptic junctions between CFs and interneuron dendrites have not been observed (Hamori and Szentagothai, 1980; Ichikawa et al., 2002; Sugihara et al., 1999). In contrast, recent studies indicate that glial cells detect glutamate that is released from CF terminals (Bergles et al., 1997; Dzubay and Jahr, 1999; Matsui and Jahr, 2003), suggesting that a major role of CFs is to influence glial cell behavior in the cerebellar cortex. However, the extent of these neuron-glia interactions and their roles in cerebellar function are poorly understood.

Two distinct types of glial cells are found in the molecular layer of the cerebellum, Bergmann glial cells (BGs) and a group of glial progenitors termed oligodendrocyte precursor cells (OPCs or NG2$^+$ cells) (Levine and Card, 1987; Palay and Chan-Palay, 1974). Although both types of glia express ionotropic glutamate receptors, only CF signaling in BGs has been examined in detail. BGs tightly ensheath excitatory synapses on PCs (Palay and Chan-Palay, 1974; Spacek, 1985), an association that helps to isolate synapses by placing glutamate transporters near sites of release and by increasing the distance for diffusion between adjacent synapses (Barbour and Hausser, 1997; Huang and Bergles, 2004). This tight ensheathment of PC synapses appears to be maintained through the activation of Ca^{2+}-permeable AMPA receptors in BGs (Iino et al., 2001). Recent studies indicate that AMPA receptors in perisynaptic BG processes are activated through ectopic fusion of synaptic vesicles outside anatomically defined active zones (Matsui and Jahr, 2003; Matsui and Jahr, 2004), and by spill out of glutamate from the synaptic cleft (Bergles et al., 1997; Dzubay and Jahr, 1999). These results indicate that BGs are not a direct target of CF axons but rather are activated as a consequence of their intimate association with CF-PC synapses.

NG2$^+$ progenitor cells are found throughout the developing and mature CNS and are responsible for generating oligodendrocytes and myelin throughout life (Levison et al., 1999; Windrem et al., 2004). NG2$^+$ cells in the hippocampus express functional AMPA receptors (Bergles et al., 2000; Lin and Bergles, 2002) that are activated at defined neuron-glia synaptic junctions (Bergles et al., 2000), in contrast to the mechanisms of receptor activation in BGs. It is not yet known if this direct form of neuron-glia signaling is ubiquitous among the entire NG2$^+$ cell population. NG2$^+$ cells in the molecular layer of the cerebellum extend numerous processes among the dendrites of PCs (Levine and Card, 1987; Palay and Chan-Palay, 1974), suggesting that they may also respond to neuronal activity in this region. However, the physiological properties of NG2$^+$ cells in this region, and their interaction with the two excitatory inputs to this region are not known.

Here, we describe a distinct CF signaling pathway in the molecular layer of the cerebellum. We find that CF stimulation induces AMPA receptor-mediated synaptic currents in NG2$^+$ glial cells located in this region, which

*Correspondence: dbergles@jhmi.edu

exhibit a sharp threshold, all-or-none behavior, and paired-pulse depression. An analysis of quantal content of CF responses suggests that a CF may form up to 70 discrete junctions with one NG2$^+$ cell and that each NG2$^+$ cell can be innervated by more than one CF. We estimated that 80% of AMPA receptors activated at these sites are Ca^{2+} permeable, based on the strong inward rectification of CF-NG2$^+$ cell currents when polyamines were present in the internal solution. CF-NG2$^+$ cell responses were less sensitive to cannabinoid or N-type Ca^{2+} channel inhibition than CF-BG responses and were remarkably stable with repeated stimulation, suggesting that they are produced through fusion at conventional release sites rather than by ectopic release. Electron microscopic analysis of physiologically identified NG2$^+$ cells revealed that anatomically defined CFs formed direct synapses with the processes of NG2$^+$ cells in the molecular layer. PF responses were also observed in NG2$^+$ cells, but these inputs were much less robust. These results indicate that CF axons also influence the behavior of NG2$^+$ cells in the cerebellum and that rapid synaptic signaling is a conserved property of this ubiquitous class of glia.

Results

NG2$^+$ Cells in Cerebellum Exhibit Properties of Glial Progenitors

To visualize NG2$^+$ cells in the cerebellum, we prepared parasagittal slices from transgenic mice that express enhanced green fluorescent protein (EGFP) under the control of the proteolipid protein (PLP) promoter, in which oligodendrocyte lineage cells express EGFP (Mallon et al., 2002). In addition to intensely fluorescent oligodendrocytes in the white matter, many small (soma diameter, 10–15 μm) weakly fluorescent cells were visible in the molecular layer of the cerebellum in these PLP-EGFP mice. These weakly fluorescent EGFP$^+$ cells were immunoreactive to antibodies against NG2 and the α receptor for the platelet-derived growth factor (PDGFαR) (Figures 1A–1F), markers of oligodendrocyte precursors (Hall et al., 1996; Nishiyama et al., 1996; Nishiyama et al., 2002). Notably, EGFP$^+$ cells were immunonegative for Pax-2, a transcription factor expressed by developing interneurons in the cerebellum (Maricich and Herrup, 1999) (Figures 1G–1I), as well as parvalbumin and NeuN, markers for interneurons in this region (Fortin et al., 1998; Weyer and Schilling, 2003) (see Figure S1 in the Supplemental Data available with this article online), indicating that NG2$^+$ cells resident in the molecular layer of the cerebellum are not immature interneurons, as has been suggested for NG2$^+$ cells in other brain regions (Aguirre and Gallo, 2004; Belachew et al., 2003).

Cerebellar NG2$^+$ Cells Are Physiologically Distinct from Neurons and Bergmann Glia

To examine the physiological properties of NG2$^+$ cells in the cerebellum, we made whole-cell recordings from EGFP$^+$ cells that were visualized in the molecular layer using combined IR-DIC and fluorescence imaging. Subsequent histological analysis of cells loaded with biocytin revealed that all EGFP$^+$ cells selected for recording were NG2$^+$ (n = 15/15 cells) (Figures 1J and 1K) and PDGFαR$^+$ (n = 5/5 cells) (data not shown). Only a single cell became labeled with biocytin, indicating that these NG2$^+$ cells were not extensively coupled through gap junctions, unlike BG (Muller et al., 1996). In whole-cell (n = 9) and perforated-patch (n = 5) current-clamp recordings, EGFP$^+$ cells had a moderate input resistance (120 ± 18 MΩ) about 4-fold higher than BG (Bergles et al., 1997), a capacitance of 23 ± 2 pF, and a resting membrane potential of –102.3 ± 0.2 mV (n = 14), close to calculated equilibrium potential for potassium (E_K = –102.5 mV). Although these cells express voltage-gated Na^+ and K^+ channels, injection of positive current did not induce action potentials or depolarizing spikes (n = 14/14 cells) (Figure 1L). In contrast, EGFP$^-$ interneurons located in the molecular layer had resting membrane potentials of –58.5 ± 0.9 mV (n = 6), fired action potentials at a high frequency when depolarized, and exhibited a morphology similar to stellate cells (n = 6/6 cells) (data not shown). These results indicate that NG2$^+$ cells in the molecular layer of the cerebellum are nonexcitable glial cells that exhibit membrane properties distinct from BG and surrounding interneurons.

Synaptic Activation of AMPA Receptors in Cerebellar NG2$^+$ Glia

NG2$^+$ cells in the molecular layer extended multiple thin processes into the neuropil among PC dendrites. To determine whether these glial cells detect glutamate released from CFs, we recorded their response to electrical stimulation of CF axons. When stimuli (15–200 μA; 100 μs) were applied to the granule cell layer, which CFs pass through before reaching PC dendrites, transient inward currents were observed in 86% of NG2$^+$ cells (94/109 cells) voltage clamped at –80 mV (Figure 2A). The average amplitude of these responses was –307 ± 55 pA (range, –56 pA to –905 pA; n = 36), in recordings that lasted for at least 5 min; the largest of these currents was capable of depolarizing NG2$^+$ cells by ~26 mV (Figure 2A). The NG2$^+$ cell responses to CF stimulation exhibited rapid rise and decay kinetics (20%–80% rise time, 406 ± 24 μs; tau decay, 1.8 ± 0.1 ms; n = 10), similar to CF EPSCs in PCs (Llano et al., 1991). Indeed, NG2$^+$ cell EPSCs were blocked by the selective AMPA receptor antagonist GYKI 53655 (50 μM; n = 5) (Figure 2B); EPSCs elicited at a holding potential of 40 mV also were blocked by the AMPA/kainate receptor antagonist NBQX (n = 31) (Figure 2C), indicating that NMDA receptors did not contribute to these responses (Wyllie et al., 1991). Cyclothiazide (CTZ), a compound that blocks desensitization of AMPA receptors and increases their apparent affinity for glutamate (Patneau et al., 1993), increased the amplitude of these responses by 99% ± 25% and slowed their decay times by 191% ± 35% (decay tau; n = 10) (Figure 2B), comparable to effects observed on neuronal EPSCs (Rammes et al., 1994; Xu-Friedman and Regehr, 2003). The rapid kinetics of NG2$^+$ cell EPSCs and their moderate enhancement by CTZ suggests that their AMPA receptors are exposed to a high concentration of glutamate for a brief period of time, similar to the glutamate concentration transient experienced by neuronal receptors in the synaptic cleft (Clements et al., 1992; Diamond and Jahr, 1997).

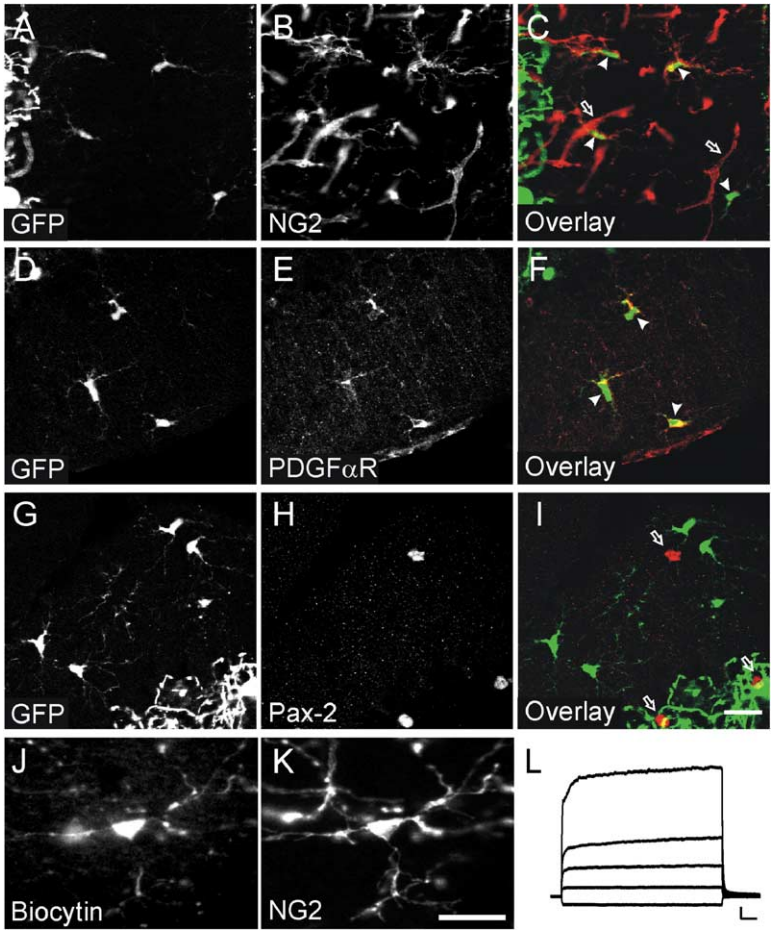

Figure 1. NG2+ Cells in the Cerebellum of PLP-EGFP Mice Express EGFP

(A–C) EGFP expression in sagittal sections of P25 cerebellum. Weakly EGFP+ cells were present in the molecular layer. Note the much brighter fluorescence from the processes of white matter oligodendrocytes in the granule cell layer, near the left border of this panel. (B) NG2 immunoreactivity in the same section as (A). (C) Overlay of (A) and (B) showing that EGFP+ cells in the molecular layer were NG2+ (arrowheads). Open arrows highlight capillaries that are also NG2+. (D–F) EGFP expression and PDGFαR immunoreactivity in the molecular layer of the cerebellum. Arrowheads in (F) indicate EGFP+/PDGFαR+ cells. (G–I) EGFP expression and Pax-2 immunoreactivity in cerebellum. EGFP+ cells did not colocalize with Pax-2. Open arrows in (I) highlight Pax-2+ nuclei of interneurons. (J) An EGFP+ NG2+ cell filled with biocytin through the whole-cell electrode. (K) NG2 immunoreactivity of region of the slice shown in (J), showing that this cell was NG2+. Scale bars for (A)–(K), 20 μm. (L) Membrane potential changes induced by current injection in a perforated-patch recording from an EGFP+ cell in molecular layer of the cerebellum. V_M = –100 mV. Current steps: –60, 60, 180, 300, and 800 pA. Scale bar, 10 mV, 50 ms. Note that this cell did not fire action potentials with strong depolarization.

AMPA Receptor-Mediated Currents in NG2+ Glia Are Mediated by CFs

CF terminals release glutamate with high probability but require many seconds to recover after release has occurred (Silver et al., 1998; Wadiche and Jahr, 2001). As a result, CF-PC EPSCs exhibit a low paired-pulse ratio (PPR) (~0.5) when two stimuli are applied within 50 ms (Hashimoto and Kano, 1998). Evoked EPSCs in NG2+ cells exhibited a PPR of 0.32 ± 0.03 (n = 20) (Figure 2D), indicating that the terminals responsible for glutamate release onto these glia also recover slowly (Figure 2E). Multivesicular release at CF-PC synapses causes saturation of AMPA receptors and leads to an underestimation of the amount of glutamate released during the first pulse of paired-pulse protocols (Wadiche and Jahr, 2001). Therefore, the smaller PPR of NG2+ cell EPSCs may indicate that their AMPA receptors are further from saturation than receptors at CF-PC synapses. Notably, the PPR of NG2+ cell EPSCs was similar to the PPR of kainate receptor currents recorded at CF-PC synapses (0.32 ± 0.02; n = 4; p = 0.45) (Figure 2F), which experience lower occupancy than AMPA receptors (Huang et al., 2004), and to CF-PC EPSCs recorded in the presence of a low-affinity AMPA receptor antagonist that prevents AMPA receptor saturation (Wadiche and Jahr, 2001). Furthermore, both NG2+ cell EPSCs and kainate receptor EPSCs at CF-PC synapses recovered from depression slowly (Figures 2E and 2F), requiring 3.2 s to reach 90% ± 3.0% (p = 0.43) (NG2+ cell EPSC) and 91% ± 1.0% (CF-PC kainate EPSC) of their initial amplitudes. These results suggest that NG2+ cell AMPA receptor currents are produced by the release of glutamate from CFs, but unlike AMPA receptors at CF-PC synapses, AMPA receptors in NG2+ cells are not saturated following this release. CF inputs with similar features were also detected in NG2+ cells in cerebellar slices prepared from mature mice (>postnatal day [P] 40) (n = 6/6 cells) (see Figure S2), indicating that this olivocerebellar synaptic input to glia matures in parallel with the CF innervation of PCs.

To address whether NG2+ cells and PCs share input from the same CFs, we made simultaneous whole-cell recordings from one PC and one NG2+ cell within single folia and measured their responses to CF stimulation. In 3/77 PC-NG2+ cell paired recordings, evoked AMPA receptor currents in NG2+ cells exhibited exactly the same threshold and all-or-none behavior as the CF EPSC in a nearby PC (Figure 3A). The NG2+ cell response was not an indirect result of PC activation, as it was unaffected when the PC was depolarized to 10 mV to reverse the direction of current flow during the CF EPSC (Figure 3B). These results indicate that NG2+ cell EPSCs occur as a direct result of glutamate release from the CF. The low incidence of coinnervation of

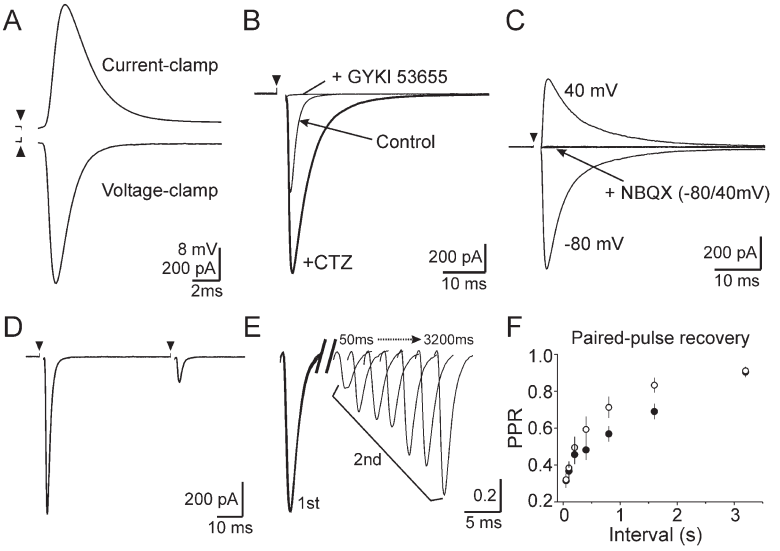

Figure 2. Evoked AMPA Receptor-Mediated Currents Recorded from Cerebellar NG2+ Cells

(A) Electrical stimulation in the granule cell layer elicited an inward current of –865 pA in an NG2+ cell (lower trace). V_M = –100 mV. In current-clamp mode, stimulation of this input depolarized the cell by 26 mV (from a resting membrane potential of –100 mV) (upper trace). (B) Evoked responses recorded from an NG2+ cell in control conditions, in the presence of cyclothiazide (CTZ; 100 μM), and in the presence of GYKI 53655 (100 μM). V_M = –80 mV. The sensitivity to both CTZ and GYKI indicates that these responses are mediated by AMPA receptors. (C) Evoked responses recorded from an NG2+ cell at V_M = –80 mV and 40 mV in control conditions and following the application of NBQX (5 μM). No outward currents were detected in NBQX, indicating that NMDA receptors did not contribute to these currents. (D) Paired-pulse depression (PPD) of evoked AMPA receptor currents recorded from an NG2+ cell. The interstimulus interval was 50 ms. V_M = –80 mV. (E) Responses of an NG2+ cell to paired stimuli applied with varying interstimulus intervals. Pairs of evoked currents with different intervals were normalized to the amplitude of the first response. Intervals: 50, 100, 200, 400, 800, 1600, or 3200 ms. (F) Plot of paired-pulse ratio (PPR) versus interstimulus interval for AMPA receptor currents recorded from NG2+ cells (filled circles) (n = 5) and CF kainate receptor EPSCs recorded from PCs in the presence of the selective AMPA receptor antagonist GYKI 53655 (100 μM) (open circles) (n = 4). Error bars are standard error of the mean. Arrowheads in (A)–(D) indicate when stimuli were applied.

neighboring NG2+ cells and PCs may indicate that most inputs to NG2+ cells occur on their processes, which extend up to 100 μm in both sagittal and transverse planes (Levine and Card, 1987; Palay and Chan-Palay, 1974).

NG2+ Cells Receive Input from Multiple CFs

In the mature cerebellum, the majority of PCs receive input from only one CF (Nishiyama and Linden, 2004; Rossi et al., 1993), an extraordinary specificity that is established over the first 2 weeks of life. The processes of individual NG2+ cells often span the dendritic arbors of four or more PCs (Figures 4A–4C), creating the opportunity for these cells to receive input from more than one CF. Indeed, 14% of NG2+ cells had EPSCs that exhibited two distinct stimulation thresholds, while 2% of NG2+ cells exhibited EPSCs with three or more thresholds (Figures 4D–4F). A greater proportion of NG2+ cells may receive multiple CF innervation in vivo, as it is difficult to ensure that every input was stimulated in these experiments, and some CF afferents may have been lost during slice preparation.

Quantal Content of CF-NG2+ Cell EPSCs

Spontaneous miniature EPSCs (mEPSCs) occurred at a low frequency (0.1–0.01 Hz) in NG2+ cells in the presence of tetrodotoxin (TTX; 1 μM) (Figure 5A). These mEPSCs had an average amplitude of –13.5 ± 4.8 pA and exhibited rapid kinetics, reaching a peak in 326 ± 64 μs (20%–80% rise time) and decaying in 1.6 ± 0.2 ms (tau decay) (n = 5 cells) (Figures 5B and 5C). The occurrence of quantal events in NG2+ cells suggests that release of a single glutamate-filled vesicle leads to rapid activation of AMPA receptors in the membranes of these glial cells. Dividing the average NG2+ cell CF

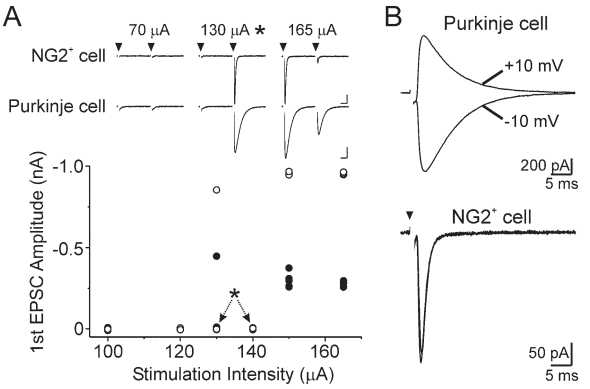

Figure 3. PCs and NG2+ Cells Receive Input from the Same CFs

(A) (Lower panel) Plot of the amplitude of the first EPSC in a paired-pulse protocol versus stimulation intensity during a simultaneous recording from one NG2+ cell (V_M = –80 mV) and one PC (V_M = –10 mV). Closed symbols correspond to responses from the NG2+ cell, and open symbols correspond to responses from the PC. Asterisk indicates failures that occurred in both NG2+ cell and PC near threshold. (Upper panel) CF responses recorded from this pair of cells at different stimulation intensities. The asterisk marks traces in which the response was evoked only following the second stimulus, corresponding to the points marked by the asterisk in the plot. Scale bars, 10 ms/50 pA in NG2+ glia EPSCs, 10 ms/200 pA for PC EPSCs. Evoked responses in this cell exhibited exactly the same threshold and all-or-none behavior. (B) Responses recorded from the PC (upper traces) and the NG2+ cell (lower traces) shown in (A) when the PC was held at V_M = –10 mV and 10 mV. The V_M of the NG2+ cell was held continuously at –80 mV. A change in the direction of current flow across the PC membrane did not alter the NG2+ cell response. Arrowheads in (A) and (B) indicate when the stimulus was applied.

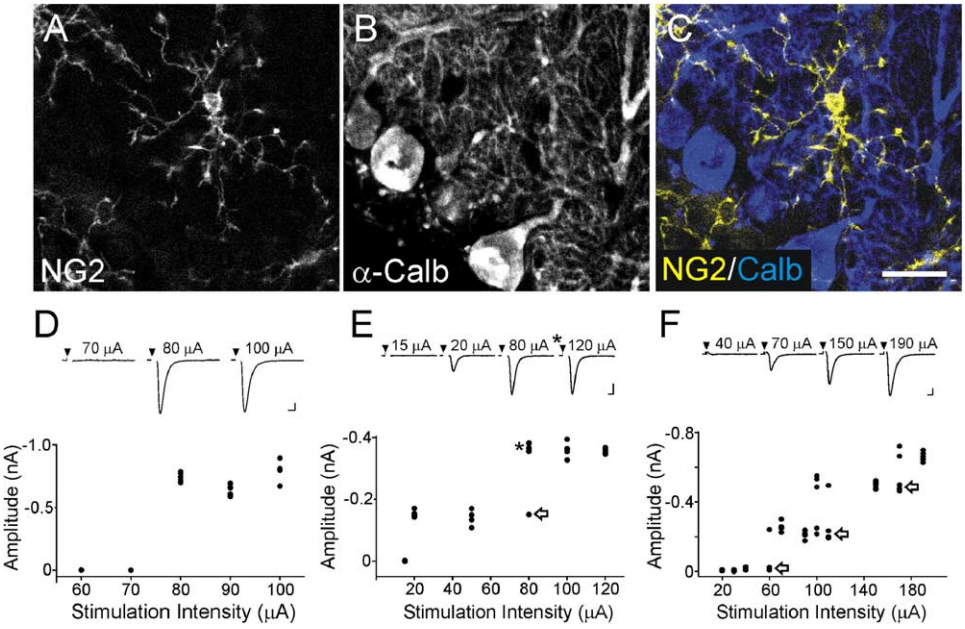

Figure 4. CF AMPA Receptor Currents in NG2+ Cells Arise from One or More CFs

(A) An NG2+ cell labeled with anti-NG2 antibody in the molecular layer of the cerebellum that extended multiple processes in the sagittal plane. (B) α-Calbindin immunoreactivity of the same region of the section shown in (A). (C) Overlay of (A) and (B) illustrating the extent of overlap between NG2+ cell processes and the dendritic arbor of PCs. Scale bar for (A)–(C), 20 μm. (D–F) Plot of NG2+ cell CF response amplitude versus stimulation intensity for three recordings (lower panels). Average responses at different stimulation intensities are shown above each plot (upper panels). The cell in (D) exhibited one threshold, the cell in (E) exhibited two thresholds, and the cell in (F) exhibited three distinct thresholds. The arrows in the lower panels of (E) and (F) indicate when the stimulation was near threshold for the next CF. Arrowheads in upper panels of (D)–(F) indicate when the stimulus was applied. Scale bars in upper panels of (D)–(F), 2 ms/100 pA.

EPSC amplitude by the average amplitude of the mEPSC provides an estimate of the number of quanta that contribute to each CF response. Because not all mEPSCs may arise from CFs (see below; Figure S3), we measured the size of individual quanta that contributed to CF EPSCs by desynchronizing evoked responses with extracellular Sr^{2+} (Oliet et al., 1996). In artificial cerebrospinal fluid (ACSF) containing Sr^{2+}, the amplitudes of evoked CF EPSCs were smaller, and quantal events occurred for ~100 ms after stimulation (Figures 5D and 5E). These evoked CF mEPSCs had an average amplitude of –11.3 ± 3.3 pA, a rise time of 345 ± 51 μs, and a decay time of 1.6 ± 0.1 ms (tau decay; n = 6), similar to the spontaneous mEPSCs (Figure 5F). If NG2+ cell AMPA receptors are not saturated by the glutamate released by the CF, as suggested by the greater paired-pulse depression of these EPSCs as compared to CF-PC EPSCs (see Figure 2D), the range of NG2+ cell CF

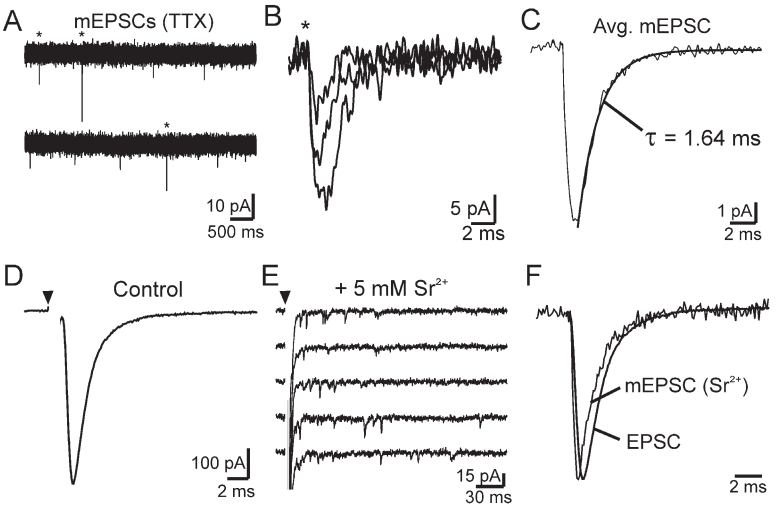

Figure 5. Determining the Quantal Content of CF-NG2+ Cell EPSCs

(A–C) mEPSCs recorded from an NG2+ cell in the presence of TTX (1 μM). Asterisks denote mEPSCs shown on an expanded timescale in (B). (C) The average waveform of mEPSCs recorded from this NG2+ cell (average of 141 events). These events were recorded in the presence of 100 μM ruthenium red to increase the frequency of spontaneous vesicle release.

(D–F) CF response from an NG2+ cell recorded under control conditions. The average amplitude was –566 pA. (E) Five evoked CF responses recorded when Ca^{2+} and Mg^{2+} in the ACSF were replaced with 5 mM Sr^{2+} ($SrCl_2$). Currents resulting from synchronous release were truncated for clarity. The arrowhead indicates when the stimulus was applied. The dark trace in (F) shows an average of 21 quantal events recorded in this cell in Sr^{2+} ACSF. The average mEPSC's amplitude was –17.6 pA, indicating that this CF EPSC had a quantal content of 32. The light trace in (F) shows the control CF EPSC in (D) scaled to the amplitude of the average mEPSC. The similar time course of these responses indicates that the 32 quanta were released synchronously.

EPSC amplitudes indicates that each NG2$^+$ cell detects the release of between 4 and 70 vesicles from one CF. A comparison of mEPSC and the CF EPSC time courses indicates that these vesicles are released in a highly synchronous manner when an action potential travels along the CF (Figure 5F). If these responses are generated at discrete CF-NG2$^+$ cell synapses, and only one vesicle fuses per site, it suggests that a CF can form as many as 70 functional synapses with one NG2$^+$ cell.

CF-NG2$^+$ Cell EPSCs Do Not Occur through Ectopic Release

At certain high-release probability synapses, vesicles can fuse at ectopic sites outside the active zone (Matsui and Jahr, 2003; Zenisek et al., 2000). At CF-PC synapses, ectopic release occurs directly opposite ensheathing BG membranes, which promotes effective activation of low-affinity AMPA receptors located in these extrasynaptic membranes (Matsui and Jahr, 2003; Matsui and Jahr, 2004). Although the sterical relationship of NG2$^+$ cell processes in the cerebellum has not been examined in detail, in the hippocampus the processes of these cells were observed in direct membrane apposition to neuronal synapses (Bergles et al., 2000; Ong and Levine, 1999), raising the possibility that CF-NG2$^+$ cell responses also could arise from ectopic release of glutamate. Ectopic release from CF terminals is more sensitive to manipulations that lower Ca^{2+} influx and slow Ca^{2+} diffusion within the terminal (Matsui and Jahr, 2003), consistent with a model in which ectopic release occurs further from sites of Ca^{2+} influx. If NG2$^+$ cell CF responses occur through ectopic release, they should exhibit a similar sensitivity to manipulations that reduce Ca^{2+} influx into CF terminals. To address this possibility, we compared the inhibition of CF responses in BGs and NG2$^+$ cells by the CB1 receptor agonist WIN 55,212-2 (WIN), a compound that inhibits CF terminal Ca^{2+} channels and decreases the amplitude of CF-PC EPSCs (Kreitzer and Regehr, 2001). At 1 μM, WIN inhibited CF-NG2$^+$ cell EPSCs by 49% ± 5% (n = 7) and increased PPR from 0.29 ± 0.03 to 0.46 ± 0.04 (n = 7; $p < 0.001$), indicating that WIN reduced the probability of glutamate release onto NG2$^+$ cells (Figures 6A–6C). This amount of WIN produced near maximal inhibition, as raising the WIN concentration 5-fold (to 5 μM) increased the inhibition of CF-NG2$^+$ cell EPSCs to only 58% ± 6% (n = 7; p = 0.09) (Figure 6F), an effect comparable to that observed at CF-PC synapses (Kreitzer and Regehr, 2001). In contrast, 1 μM WIN inhibited CF-BG-evoked responses by 95% ± 2% (n = 6) (Figures 6D–6F), significantly greater than that observed for CF-NG2$^+$ cell EPSCs ($p < 0.001$ for both 1 μM and 5 μM WIN) (Figure 6F). The glutamate transporter antagonist TBOA (DL-threo-b-benzyloxyaspartic acid) was applied at the end of these experiments to show that the CF-BG response remaining in NBQX was mediated by glutamate transporters (Bergles et al., 1997).

Recent studies by Matsui and Jahr (2004) indicate that ectopic release from CFs shows a greater dependence on Ca^{2+} influx through N-type Ca^{2+} channels than conventional release at active zones. To provide further evidence that CF-NG2$^+$ cell signaling is distinct from ectopic release, we measured the sensitivity of CF-NG2$^+$ cell EPSCs to block by the selective N-type Ca^{2+} channel antagonist ω-conotoxin GVIIA. As shown in Figures 6G–6I, CF-NG2$^+$ cell responses recorded in ACSF containing 2 mM Ca^{2+}, conditions used in the studies of Matsui and Jahr (2004), were inhibited by only 36% ± 6% (n = 7) by 1 μM ω-conotoxin GVIIA, significantly lower than that reported for CF-BG responses (~83%), but similar to that reported for CF-PC responses (~36%) when saturation was prevented with γ-DGG (Matsui and Jahr, 2004). The comparable sensitivity of neuronal and NG2$^+$ cell synaptic responses to N-type Ca^{2+} channel and cannabinoid-mediated inhibition suggests that CF EPSCs in NG2$^+$ cells occur as a result of vesicle fusion at conventional, rather than ectopic release sites.

PF Inputs to NG2$^+$ Cells

The number of PF axons greatly exceeds the number of CF axons in the molecular layer of the cerebellum, raising the question of whether NG2$^+$ cells also receive PF input. When stimuli were applied within the molecular layer, small inward currents were evoked in 15/15 NG2$^+$ cells. These responses exhibited paired-pulse facilitation (PPR: 2.07 ± 0.13; $p < 0.001$ when compared to CF-NG2$^+$ cell EPSCs) and graded increases in amplitude with increasing stimulation intensity (see Figure S3A). These responses had a rise time of 453 ± 25 μs and a decay time of 1.86 ± 0.23 ms (tau decay; n = 15), comparable to CF EPSCs, and were also blocked by NBQX (see Figure S3B). The graded nature of these responses and their facilitation with paired stimuli suggest that these responses were produced by glutamate released from PF axons. However, it was difficult to study these inputs in isolation, because the CF input was typically recruited as the stimulation intensity increased, obscuring the much smaller PF response. We conclude from these data that, although NG2$^+$ cells are capable of receiving both CF and PF input, the CF input dominates. It is unlikely that PFs contributed to the multiple CF responses seen following stimulation in the granule cell layer (illustrated in Figure 4), because the PPR of dual CF responses was the same as those arising from a single CF (PPR: single CF EPSC, 0.29 ± 0.04; dual CF EPSCs, 0.28 ± 0.03; n = 9; p = 0.4).

CFs Form Synaptic Junctions with NG2$^+$ Cells

CF EPSCs could be reliably evoked in NG2$^+$ cells for >30 min with repeated stimulation (at 0.67 Hz), suggesting that these currents are generated at stable junctions where vesicles can be released and recycled. Using electron microscopy to examine the relationship between CF terminals and these glial cells, we followed biocytin-labeled processes of physiologically characterized NG2$^+$ cells that responded to CF stimulation. Anatomically defined synapses were observed along the processes of four NG2$^+$ cells examined in serial sections. Synaptic junctions were identified by the rigid parallel apposition of the membrane of the biocytin-labeled process and the vesicle-containing bouton, the accumulation of synaptic vesicles at such sites together with presynaptic dense projections, and the accumulation of electron opaque material in the extracellular space (Figure 7). In all respects, such junctions

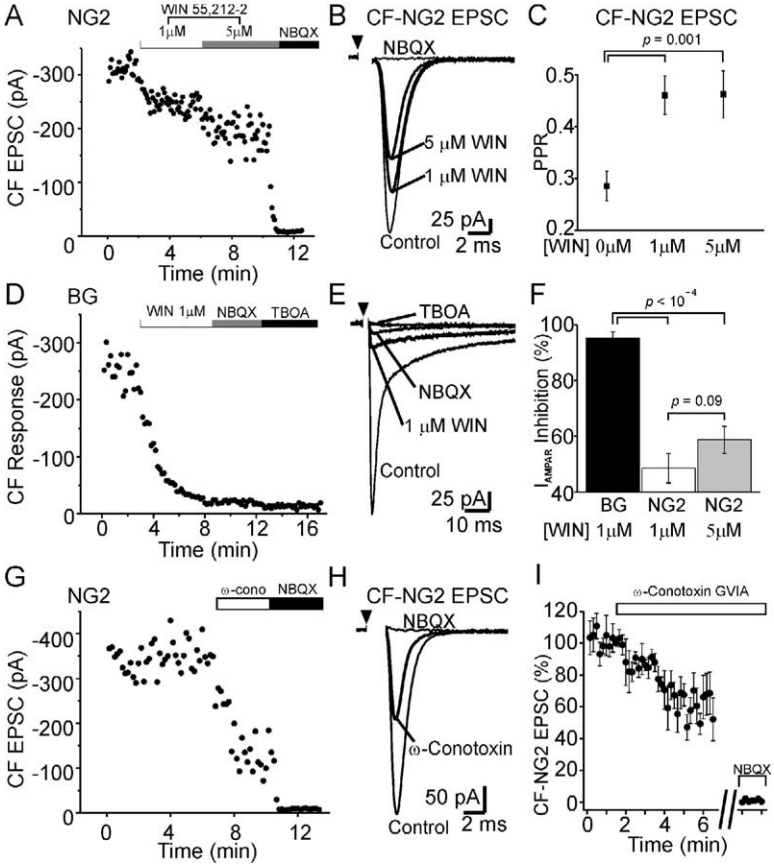

Figure 6. CF Responses in NG2+ Cells and BGs Exhibit Differential Sensitivity to Cannabinoids and ω-Conotoxin GVIA

(A) Plot of the peak amplitude of CF-NG2+ cell EPSCs over time during one representative experiment. The bars above the plot indicate the duration of drug application.

(B) Average traces of ten consecutive CF-NG2+ cell EPSCs recorded during each condition for the experiment shown in (A).

(C) Plot of the paired-pulse ratio (P2/P1; interstimulus interval, 50 ms) under control conditions and in the presence of 1 μM and 5 μM WIN (WIN 55-212,2) (n = 7). The increase in PPR indicates that WIN decreased release probability. Error bars are standard error of the mean.

(D) Plot of the peak amplitude of CF-BG EPSCs over time during one representative experiment. The bars above the plot indicate the duration of drug application. Note the greater inhibition of these responses by 1 μM WIN. The glutamate transporter antagonist TBOA was applied at the end of the experiment to show that the current remaining in NBQX was mediated by glutamate transporters.

(E) Average of ten consecutive CF-BG responses recorded during each condition for the experiment shown in (D).

(F) Summary of the effects of WIN 55,212-2 on CF-BG (n = 9) and CF-NG2+ cell (n = 7) responses. Arrowheads in (B) and (E) indicate when the stimulus was applied. Error bars are standard error of the mean.

(G) Plot of the peak amplitude of NG2+ cell CF EPSCs during one experiment showing the inhibition of the response by ω-conotoxin GVIA (1 μM).

(H) Average of ten consecutive CF-NG2+ cell responses recorded during each condition for the experiment shown in (D).

(I) Plot of the average amplitudes of CF-NG2+ cell responses from seven experiments illustrating that ω-conotoxin GVIA reduced CF-NG2+ cell EPSCs to ~64% of control. Error bars are standard error of the mean.

were similar to those established by CF and PF boutons with PCs and interneurons. After sectioning about 5%–20% of each of these four cells, a total of 44 synapses were observed (22 on cell 1, 6 on cell 2, 11 on cell 3, and 5 on cell 4). No synapses were found on the cell bodies of NG2+ cells, although they were not completely sectioned. The size of the boutons (long axis, 0.3–2 μm) and the length of the synaptic junctions (0.1–

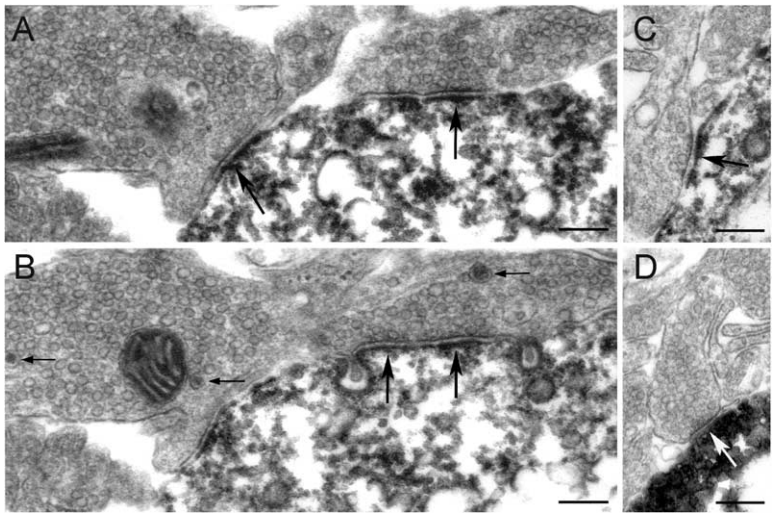

Figure 7. Electron Microscopic Analysis of Synaptic Junctions on NG2+ Cells

(A and B) Serial sections from a cerebellar slice in which a single NG2+ cell in the molecular layer was filled through the whole cell electrode with biocytin. Visible in these micrographs are two large CF boutons, each making synaptic junctions (arrows) with a lightly biocytin-labeled (HRP reaction product) process of an NG2+ cell that responded to CF stimulation. The boutons contain a high density of small clear vesicles and large granulated vesicles (small arrows). (C and D) Small boutons forming synaptic junctions (arrows) with two different NG2+ cells. The bouton in (C) contains few vesicles and innervates the same cell as shown in (A) and (B), whereas the one in (D) contains a high density of vesicles like the large boutons in (A) and (B). These inputs may correspond to small CF boutons or PF boutons. Scale bars, 0.2 μm.

0.6 μm) varied greatly from synapse to synapse and from cell to cell. Two cells received only small synapses within the area examined, while the other cells also received synapses from large boutons containing densely packed small clear synaptic vesicles, numerous large granulated and coated vesicles, and prominent presynaptic specializations, reminiscent of CF terminals on PCs, (Hamori and Szentagothai, 1980; Palay and Chan-Palay, 1974). The origin of the small boutons could not be directly determined, but several were also densely packed with vesicles (Figure 7D) like CF boutons; therefore, they may represent smaller CF terminals, PF terminals, or a mixture of both. Notably, synapses on NG2$^+$ cell processes were not wrapped by Bergmann glial lamellae. Biocytin-labeled processes of NG2$^+$ cells were also in direct membrane apposition with boutons that made no synaptic junctions, as well as with PF axons, Bergmann glial processes, and interneuron dendrites. This diverse association with neuronal and nonneuronal elements may allow these glia to have a wide influence in this region.

CF Activation of Ca^{2+}-Permeable AMPA Receptors in NG2$^+$ Cells

The largest CF EPSCs depolarized NG2$^+$ cells to ~–74 mV (see Figure 3A), well below activation range of even low voltage-activated Ca^{2+} channels (Huguenard, 1996). To better understand the potential of CF inputs to modulate the behavior of these glial cells, we examined whether NG2$^+$ cell AMPA receptors were Ca^{2+} permeable. AMPA receptors formed without edited GluRB (GluR2) subunits are permeable to Ca^{2+} and exhibit inwardly rectifying current-voltage (*I-V*) relationships due to channel block by intracellular polyamines (Donevan and Rogawski, 1995). When spermine (100 μM) was included in the electrode solution, current flow through these AMPA receptors was greatly reduced at 40 mV when compared to –40 mV (n = 7), causing CF-NG2$^+$ cell EPSCs to exhibit profound inward rectification (Figures 8A and 8B). NG2$^+$ cell EPSCs recorded without spermine in the electrode solution exhibited a linear *I-V* relationship (n = 4) (Figures 8A and 8B), indicating that this rectification was due to intracellular block by polyamines. The amplitude ratio of EPSCs at 40 mV (spermine/control) was 0.2, indicating that up to 80% of the NG2$^+$ cell AMPA receptors activated by CFs are Ca^{2+} permeable. These results indicate that neurons in the inferior olive stimulate Ca^{2+} influx into cerebellar NG2$^+$ cells by activating Ca^{2+}-permeable AMPA receptors at direct CF-NG2$^+$ cell synapses.

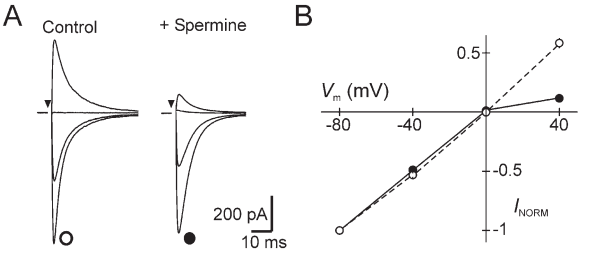

Figure 8. CF-NG2$^+$ Cell EPSCs Are Mediated by Calcium-Permeable AMPA Receptors

(A) CF-NG2$^+$ cell EPSCs recorded from an NG2$^+$ cell at V_M = –80, –40, 0, and 40 mV with an internal solution lacking spermine (left traces; control). CF NG2$^+$ cell EPSCs recorded from a different cell with an internal solution that contained 100 μM spermine (right traces; spermine). Note that spermine reduced the amplitude of responses evoked at positive holding potentials. Cyclothiazide (100 μM) was present in the ACSF for these experiments. Arrowheads indicate when the stimulus was applied.

(B) Current-voltage (*I-V*) plots showing the average amplitudes of CF-NG2$^+$ cell AMPA receptor currents recorded with spermine (filled circles; n = 7) and without spermine (open circles; n = 4) in the intracellular solution. Evoked responses were normalized to their amplitude at V_M = –80. Error bars are standard error of the mean.

Discussion

CF axons provide one of the two major glutamatergic afferents to the cerebellum and are essential for cerebellar plasticity. We find that the same CFs that innervate PCs in the molecular layer of the cerebellum also form extensive synaptic junctions with NG2$^+$ cells, a distinct class of nonexcitable glia. Release of glutamate from CF terminals at these neuron-glia synapses occurs with high probability and triggers rapid but momentary activation of AMPA receptors in NG2$^+$ cell membranes, similar to synaptic currents generated at CF-PC synapses. This innervation of NG2$^+$ cells appears to be both highly specific and robust. Although basket and stellate interneurons are much more abundant than NG2$^+$ cells in this region and have extensive dendritic arbors, they receive little or no CF input (Desclin, 1976; Hamori and Szentagothai, 1980; Ichikawa et al., 2002; Jorntell and Ekerot, 2003). Based on the quantal content of CF responses, the density of CF synapses on NG2$^+$ cells is about half of that observed on PCs, when the number of inputs is scaled to cell size (NG2$^+$ cell: 25 synapses/23 pF = 1.1 synapses/pF; PC: ~1,000 synapses/425 pF = 2.4 synapses/pF) (Otis et al., 1997; Rossi et al., 1993; Silver et al., 1998). Furthermore, this form of neuron-glial cell innervation was not restricted to NG2$^+$ cells located in particular folia or to early developmental times. Notably, PF input was also observed in these cells, although it appeared much less robust than the CF input. If these neuron-glia synaptic junctions are widespread, why have they not been observed in previous anatomical studies of this region? Although the somata of these glial cells have been described in EM-level analyses of the cerebellum (Levine and Card, 1987; Palay and Chan-Palay, 1974; Peters et al., 1991), CF inputs occurred primarily, if not exclusively, on NG2$^+$ cell processes, which are very thin and move in a tortuous path through the neuropil. In addition, these processes lack conspicuous GFAP filaments, creating difficulties for unambiguous identification. Notably, CF axons extend fine collaterals in the transverse plane that often enlarge to form varicosities on small cells (Sugihara et al., 1999). Although these cells were presumed to be interneurons, the present results suggest that some of these "terminal branchlets" may be the source of NG2$^+$ cell innervation. It is also possible that innervation of NG2$^+$ cells may be induced or enhanced in vitro following preparation of tissue slices. If so, these junctions must be formed rapidly

and then stabilize, as the amplitudes of CF NG2+ cell EPSCs were not larger in slices that had been maintained longer in vitro, and in several long-duration recordings the amplitude of CF EPSCs remained stable for more than 1 hr.

CFs Use Distinct Mechanisms to Communicate with NG2+ Cells and Bergmann Glia

CFs also trigger the activation of AMPA receptors in BGs (Bergles et al., 1997), astrocyte-like cells that ensheath PC synapses. These receptors are activated primarily through release at ectopic sites in CF terminals (Dzubay and Jahr, 1999; Matsui and Jahr, 2003; Matsui and Jahr, 2004). In contrast, NG2+ cell processes do not ensheath CF-PC synapses and are thus unlikely to be activated by ectopic release. Consistent with this observation, CF-NG2+ cell responses were enhanced only ~2-fold when the affinity of AMPA receptors was enhanced by CTZ, while Bergmann glial responses are enhanced more than 8-fold by CTZ (Dzubay and Jahr, 1999); when AMPA receptor affinity is enhanced by CTZ, receptors in perisynaptic BG membranes respond to both ectopic release and glutamate that spills out of the CF-PC synaptic cleft, resulting in greater potentiation. Ectopic release onto BGs is triggered primarily by Ca^{2+} influx through N-type Ca^{2+} channels (Matsui and Jahr, 2004) and is more sensitive to manipulations that restrict diffusion of Ca^{2+} within the terminal (Matsui and Jahr, 2003). Notably, CF AMPA receptor currents in NG2+ cells were inhibited less than CF-BG responses by CB1 cannabinoid receptor activation and by the N-type Ca^{2+} channel antagonist ω-conotoxin GVIA. These data are in accordance with prior studies showing that CB1 receptors preferentially inhibit N-type Ca^{2+} channels (Brown et al., 2004), while release at CF-PC synapses is mediated primarily by P/Q-type channels (Regehr and Mintz, 1994). These results indicate that CFs rely on distinct mechanisms to communicate with these two different classes of glial cells: BGs are activated by ectopic release at CF-PC synapses, while NG2+ cells are a direct synaptic target of CF axons.

The Identity and Fate of NG2+ Cells in the Adult CNS

The developing nervous system contains a large population of proliferating NG2+ and PDGFαR+ cells that migrate from the subventricular zones (SVZ) to populate both gray and white matter regions before maturing into myelinating oligodendrocytes (LeVine and Goldman, 1988; Levison et al., 1993). Unlike most progenitors, NG2+/PDGFαR+ cells are still observed in the adult CNS, where they adopt a more complex morphology, exhibit lower rates of proliferation, and have a reduced ability to migrate (Levine et al., 2001). Lineage tracing using low-titer retroviral infection of the early postnatal SVZ revealed the appearance of some homogeneous clusters of NG2+ cells in the adult brain, rather than mixed clones of NG2+ cells and oligodendrocytes (Levison et al., 1999), suggesting that these cells may not be irrevocably committed to an oligodendrocyte fate. Consistent with these observations, NG2+ cells removed from the postnatal gray and white matter can develop into neurons in vitro (Belachew et al., 2003; Kondo and Raff, 2000) and in vivo (Shihabuddin et al., 2000) when exposed to serum or basic fibroblast growth factor, suggesting that they retain a certain developmental plasticity.

Recent studies have suggested that some NG2+ cells in both the developing SVZ and gray matter may serve as progenitors for interneurons, based on the expression of EGFP by interneurons in CNPase-EGFP mice (Belachew et al., 2003), TOAD-64 by NG2+ cells in the dentate gyrus (Belachew et al., 2003), and the transcription factor Er81 by NG2+ cells within the rostral migratory stream (Aguirre and Gallo, 2004); some NeuN+ proliferating cells in the adult cortex have also been shown to exhibit and NG2 immunoreactivity (Dayer et al., 2005). If NG2+ cells in the molecular layer of the cerebellum are developing interneurons, these CF inputs may provide a transient instructive role for further differentiation. However, mixed interneuron/NG2+ cell clones were not observed in retroviral tracing studies (Levison et al., 1999; Zhang and Goldman, 1996), and analysis of mRNA expression by resident NG2+ cells in gray matter indicates that they do not express neurofilament mRNA (Ye et al., 2003). In accordance with these latter observations, NG2+ cells in the postnatal and adult cerebellar molecular layer do not express Pax-2, a transcription factor expressed by all interneuron progenitors in this region (Maricich and Herrup, 1999), or BM88, a cell cycle regulator expressed by progenitors committed to become neurons (Koutmani et al., 2004). Furthermore, cerebellar NG2+ cells exhibited a much more negative resting potential than neurons or neuronal progenitors (Overstreet et al., 2004; Wang et al., 2003), and they did not fire spikes in response to depolarizing current injection. These results are consistent with the hypothesis that postmigratory NG2+ cells in the gray matter are restricted to a glial fate. Unlike astrocytes, NG2+ cells do not express glutamate transporters, do not exhibit a high resting conductance to K^+, do not wrap around capillaries, do not express GFAP, and are not extensively coupled by gap junctions (Lin and Bergles, 2002; Wyllie et al., 1991); these cells also do not express markers of mature oligodendrocytes or microglia (Nishiyama et al., 1999). These observations suggest that the majority of NG2+ cells resident in the mature CNS represent a class of macroglia distinct from astrocytes and oligodendrocytes (Butt et al., 2002; Dawson et al., 2000; Nishiyama et al., 1999; Peters, 2004).

Functions of CF-NG2+ Cell Signaling

CF responses were observed in >80% of NG2+ cells in the molecular layer of the cerebellum, suggesting that there is a concerted effort to influence the behavior of these glia. Unitary CF responses depolarized NG2+ cells by up to 26 mV but failed to induce regenerative activity such as Na^+- or Ca^{2+}-dependent spikes; due to the high membrane potential (–100 mV) of NG2+ cells, depolarizations of this magnitude were not sufficient to induce substantial activation of voltage-gated channels. Although the voltage excursion in thin processes may be greater, the AMPA receptors activated at CF-NG2+ cell synapses exhibited pronounced inward rectification characteristic of Ca^{2+}-permeable receptors (Donevan and Rogawski, 1995) when spermine was

present in the pipette solution. AMPA receptors in these glia may therefore serve as a direct route for Ca^{2+} influx rather than a current source for depolarization, similar to AMPA receptors in BGs (Iino et al., 2001). The high rate of CF activity in vivo (Mariani and Changeux, 1981) suggests that Ca^{2+} transients in $NG2^+$ cell processes are likely to occur at a frequency greater than 1 Hz, raising the possibility that these cells provide some ongoing trophic support to CFs, or that the absence of CF activity might induce changes in $NG2^+$ cell behavior, as has been suggested for CF regulation of PC output (Medina et al., 2002). Retrograde signaling at a subset of synapses has been shown to influence synaptic efficacy at other synapses formed by the same axon (Casadio et al., 1999; Cash et al., 1996). If $NG2^+$ cells release neuromodulators in response to a rise in cytosolic Ca^{2+} (Barres et al., 1990), they may influence CF excitation of PCs or help to maintain CF-PC synapses, as $NG2^+$ cells and PCs share input from the same CF.

While most PCs in the mature cerebellum receive input from only one CF (Nishiyama and Linden, 2004), many $NG2^+$ cells received input from multiple CFs, consistent with the orientation of their processes across dendritic fields of multiple PCs in both sagittal and transverse planes. This greater convergence of CF innervation may allow the relatively few $NG2^+$ cells present in the molecular layer to monitor CF activity throughout the cerebellar cortex. $NG2^+$ cells in the hippocampus have been shown to form synapses with glutamatergic pyramidal neurons (Bergles et al., 2000), suggesting that rapid communication through direct synapses is a common form of neuron-$NG2^+$ cell signaling in the brain.

$NG2^+$ glia cultured from the developing CNS, termed O-2A cells or OPCs, express both AMPA and kainate receptors (Gallo et al., 1994; Patneau et al., 1994), and prolonged activation of these receptors in vitro induces changes in gene expression (Knutson et al., 1997; Pende et al., 1994), decreases their proliferation, and prevents these cells from maturing into oligodendrocytes (Gallo et al., 1996). Although it is likely that $NG2^+$ cells experience much more transient activity under physiological conditions, these results raise the possibility that AMPA receptor signaling may influence the development and fate of these progenitors. Consistent with this hypothesis, $NG2^+$ cells in cerebellar slices that were cultured in an AMPA/kainate receptor antagonist exhibited greater numbers of $NG2^+$ cells (Yuan et al., 1998). Thus, CF innervation of $NG2^+$ cells may provide an inhibitory signal to prevent their further differentiation in this region of the cerebellar cortex that is devoid of myelin. In the white matter, $NG2^+$ cells make contact with nodes of Ranvier (Butt et al., 1999), raising the possibility that these cells influence the formation or maintenance of the node, or that ion flux through $NG2^+$ cell membranes alters axonal excitability (Wyllie et al., 1991). Although the molecular layer lacks similar nodal regions, this close association between $NG2^+$ cells and axons is maintained. The challenge for future studies will be to manipulate AMPA receptors selectively in $NG2^+$ cells to address the specific role of this neuron-glial communication in regulation of their development and function in intact neural circuits.

Experimental Procedures

Slice Preparation and Cell Identification

PLP-EGFP mice were generated as reported (Mallon et al., 2002). Parasagittal slices (250 μm) from P16 to P25 PLP-EGFP mice were obtained from cerebellar vermis and maintained as previously described (Lin and Bergles, 2004), in strict accordance with a protocol approved by the Animal Care and Use Committee at Johns Hopkins University. Slices for experiments on Bergmann glia were obtained from younger mice (P8–P12), prior to the establishment of extensive cell-cell coupling. For analysis of PF input to $NG2^+$ cells, coronal slices of cerebellum (250 μm) were made to provide better preservation of PF axons and to isolate this input from the CF input. Slices were transferred to perspex chamber mounted on the fixed stage of an upright microscope (Zeiss Axioskop FS2) equipped with both DIC optics and a filter set for fluorescence imaging of EGFP. Experiments were performed at 22°C–24°C. Cells were visualized using 770 nm and 488 nm light, with a 40× water immersion objective (Zeiss Acroplan 40× IR) and two CCD cameras (Sony XC-73 and XC-EI30). Two CCD camera controllers (Hamamatsu C-2400) were used to adjust image quality in IR-DIC and EGFP channels. An image combiner (MicroImage PIX/2) was used to visualize and patch $EGFP^+$ cells.

Electrophysiology

Whole-cell recordings were made from NG2 glia using conventional techniques, as described (Lin and Bergles, 2004), in ACSF composed of the following: NaCl (119 mM), KCl (2.5 mM), $CaCl_2$ (2.5 mM), $MgCl_2$ (1.3 mM), NaH_2PO_4 (1 mM), $NaHCO_3$ (26.2 mM), and glucose (11 mM). The electrode solution consisted of the following: $CsCH_3SO_3H$ (CsMeS) (100 mM), tetraethylammonium (TEA) hydroxide (20 mM), HEPES (20 mM), EGTA (10 mM), Na-ATP (2 mM), and Na-GTP (0.2 mM) (pH 7.3). QX-314 chloride (1 mM; Alomone Labs) was added to the electrode solution used on cerebellar PCs. For current-clamp experiments, KCH_3SO_3H (KMeS) replaced CsMeS in the electrode solution, and TEA was omitted. Evoked responses were elicited with a constant-current stimulator (Digitimer DS3) using a bipolar stainless steel electrode (Frederick Haer Co., Bowdentown, Maine; tip separation, 150 μm) that was placed in the granule cell layer; CF inputs to BGs were evoked using a theta glass capillary electrode (Bergles et al., 1997). The stimuli used to elicit evoked release varied between 15 and 200 μA and were 100 μs in duration. Pipette resistances were 2.5–3.5 MΩ, and recordings of evoked and spontaneous currents were made without series resistance compensation. Membrane potentials have been corrected for the error resulting from the liquid junction potentials. Unless otherwise noted, the holding potential (V_M) was −80 mV. Gabazine (SR-95531; Tocris; 5 μM) and picrotoxin (Sigma; 100 μM) were always present in the bath during recordings, and the following agents were added as indicated: TTX (Alomone Lab), 1 μM; CTZ (Tocris), 100 μM; GYKI 53655 or GYKI 52466 (both Sigma), 100 μM; 2,3-dihydroxy-6-nitro-7-sulphamoyl-benzo(F)quinoxaline (NBQX; Tocris), 5 μM; ruthenium red (Sigma), 100 μM. GYKI 53655 (100 μM) was used to isolate kainate receptor-mediated CF-PC EPSCs (Huang et al., 2004). We performed perforated-patch recordings using a KMeS-based internal solution containing 5 μg/ml gramicidin-A (Sigma) (Lin and Bergles, 2004). The membrane resistance of $NG2^+$ cells was >1 GΩ when recordings were made with the CsMeS-based solution.

Analysis

Evoked and spontaneous currents were recorded using a MultiClamp 700A amplifier (Axon Instruments, Union City, CA), filtered at 2 kHz, digitized at 50 kHz, and recorded to disk using pClamp9 software (Axon Instruments) or stored continuously to tape (CDAT-4, Cygnus Technology, Delaware Water Gap, PA). Data were analyzed offline using Clampfit (Axon Instruments), Origin (OriginLab Corp., Northampton, MA), and Mini analysis (Synaptosoft Inc., Decatur, GA) software. Data are expressed as mean ± standard error of the

mean, and statistical significance was determined using the paired or unpaired Student's t test, as appropriate. The PPR was determined by dividing the average peak amplitude of the second response (P2) by the peak amplitude of the first response (P1). The decay time (tau) of events was measured by fitting the response with a single exponential using the logistic equation. Stimulus artifacts have been truncated for clarity.

Histology

Biocytin (0.15% w/v; Molecular Probes) was included in the electrode and allowed to diffuse into the cell for >5 min, the seal was destroyed with large negative current pulses, and the electrode was removed. For these labeling experiments, only one cell was recorded in each slice. The slice was then sandwiched between two filter discs and placed in ice-cold fixative solution consisting of 4% paraformaldehyde in phosphate-buffered saline (PBS) with 0.2% w/v picric acid. Slices were kept in this solution overnight at 4°C, then washed in PBS, cryoprotected in sucrose, and frozen with 2-methyl-butane in OCT compound (Electron Microscopy Sciences,). Slices were blocked and resectioned at 40 μm on a cryostat (Zeiss; 500OM), or at 50 μm on a vibratome following gelatin embedding. For labeling, slices were treated with 0.3% Triton X-100, and nonspecific antibody reaction was blocked with 5% donkey serum. Biocytin was visualized with Cy3-conjugated (1:2000), Cy5-conjugated (1:500; Jackson ImmunoResearch), or AMCA-conjugated streptavidin (1:1000; Vector Lab). The rabbit anti-NG2 antibody (1:1500), guinea pig anti-NG2 antibody (1:1000), and rabbit anti-PDGFαR antibody (1:1000) were generously provided by W.B. Stallcup (Tillet et al., 1997) and A. Nishiyama. The anti-NG2 antibodies label both NG2 glia and some perivascular cells surrounding capillaries. Chicken anti-GFP antibody (1:5000) and mouse anti-NeuN antibody (1:500) (both from Chemicon), mouse anti-parvalbumin antibody (clone PARV-19; 1:4000) and mouse anti-calbindin antibody (1:3000) (both from Sigma), and rabbit anti-Pax-2 antibody (1:2000; Zymed) were used when appropriate. Immunoreactivity to different antigens was detected with Alexa (Molecular Probes)-, Cy3-, or Cy5-conjugated anti-rabbit, anti-guinea pig, or anti-mouse IgG and Cy2-conjugated anti-chicken IgY secondary antibodies (1:500; Jackson ImmunoResearch). Fluorescent images were collected with a Noran Oz confocal microscope (Noran, Middleton, WI) attached to an upright microscope (Zeiss Axioskop FS2) using a 40× water immersion objective, Kr-Ar (488 nm, 568 nm) and red HeNe (633 nm) lasers, and FITC (500–550 nm band pass), Cy3 (590 nm band pass), and Cy5 (660 nm long pass) filter sets. Control sections incubated with secondary antibody alone did not result in labeling of cells.

Electron Microscopy

For electron microscopic analysis, slices were fixed in 4% paraformaldehyde and 1.25%–2.25% glutaraldehyde in PBS with ~0.2% w/v picric acid, embedded in gelatin, resectioned at 50 μm on a vibratome, and rinsed in 0.1 M PB. Biocytin was visualized by avidin biotinylated horseradish peroxidase complex "elite" kit (1:50; Vector Lab) at 4°C overnight. Peroxidase enzyme reaction was carried out in a solution of 0.01% hydrogen peroxide and 0.05% 3′,3′-diaminobenzidine tetrahydrochloride (Sigma). Sections from one cell were freeze thawed following cryoprotection in sucrose before visualizing biocytin. Following rinsing, the sections were postfixed for 40 min in 1% OsO_4 in 0.1 M PB, dehydrated, and embedded in Durcupan ACM (Fluka) resin. To enhance contrast for electron microscopy, the sections were stained with 1% uranyl acetate in 70% ethanol for 30 min. Serial sections were cut at ~70 nm on an ultramicrotome, mounted on pioloform-coated single-slot copper grids, and contrasted with lead citrate.

Supplemental Data

The Supplemental Data include three supplemental figures and can be found with this article online at http://www.neuron.org/cgi/content/full/46/5/773/DC1/.

Acknowledgments

The authors thank Dr. W. Stallcup for antibodies to NG2 and PDGFα receptor and Dr. A. Nishiyama for antibodies to NG2. We also thank Jennifer Ziskin for comments on the manuscript and Ms. Wai Yee Suen for assistance with some of the immunocytochemistry. This work was supported in part by a Basil O'Connor Starter Scholar Research Award from the March of Dimes; D.E.B. is an Alfred P. Sloan Research Fellow.

Received: January 10, 2005
Revised: April 4, 2005
Accepted: April 20, 2005
Published: June 1, 2005

References

Aguirre, A., and Gallo, V. (2004). Postnatal neurogenesis and gliogenesis in the olfactory bulb from NG2-expressing progenitors of the subventricular zone. J. Neurosci. *24*, 10530–10541.

Barbour, B., and Hausser, M. (1997). Intersynaptic diffusion of neurotransmitter. Trends Neurosci. *20*, 377–384.

Barres, B.A., Koroshetz, W.J., Swartz, K.J., Chun, L.L., and Corey, D.P. (1990). Ion channel expression by white matter glia: the O-2A glial progenitor cell. Neuron *4*, 507–524.

Belachew, S., Chittajallu, R., Aguirre, A.A., Yuan, X., Kirby, M., Anderson, S., and Gallo, V. (2003). Postnatal NG2 proteoglycan-expressing progenitor cells are intrinsically multipotent and generate functional neurons. J. Cell Biol. *161*, 169–186.

Bergles, D.E., Dzubay, J.A., and Jahr, C.E. (1997). Glutamate transporter currents in Bergmann glial cells follow the time course of extrasynaptic glutamate. Proc. Natl. Acad. Sci. USA *94*, 14821–14825.

Bergles, D.E., Roberts, J.D., Somogyi, P., and Jahr, C.E. (2000). Glutamatergic synapses on oligodendrocyte precursor cells in the hippocampus. Nature *405*, 187–191.

Brown, S.P., Safo, P.K., and Regehr, W.G. (2004). Endocannabinoids inhibit transmission at granule cell to Purkinje cell synapses by modulating three types of presynaptic calcium channels. J. Neurosci. *24*, 5623–5631.

Butt, A.M., Duncan, A., Hornby, M.F., Kirvell, S.L., Hunter, A., Levine, J.M., and Berry, M. (1999). Cells expressing the NG2 antigen contact nodes of Ranvier in adult CNS white matter. Glia *26*, 84–91.

Butt, A.M., Kiff, J., Hubbard, P., and Berry, M. (2002). Synantocytes: new functions for novel NG2 expressing glia. J. Neurocytol. *31*, 551–565.

Casadio, A., Martin, K.C., Giustetto, M., Zhu, H., Chen, M., Bartsch, D., Bailey, C.H., and Kandel, E.R. (1999). A transient, neuron-wide form of CREB-mediated long-term facilitation can be stabilized at specific synapses by local protein synthesis. Cell *99*, 221–237.

Cash, S., Zucker, R.S., and Poo, M.M. (1996). Spread of synaptic depression mediated by presynaptic cytoplasmic signaling. Science *272*, 998–1001.

Clements, J.D., Lester, R.A., Tong, G., Jahr, C.E., and Westbrook, G.L. (1992). The time course of glutamate in the synaptic cleft. Science *258*, 1498–1501.

Dawson, M.R., Levine, J.M., and Reynolds, R. (2000). NG2-expressing cells in the central nervous system: are they oligodendroglial progenitors? J. Neurosci. Res. *61*, 471–479.

Dayer, A.G., Cleaver, K.M., Abouantoun, T., and Cameron, H.A. (2005). New GABAergic interneurons in the adult neocortex and striatum are generated from different precursors. J. Cell Biol. *168*, 415–427.

Desclin, J.C. (1976). Early terminal degeneration of cerebellar climbing fibers after destruction of the inferior olive in the rat. Synaptic relationships in the molecular layer. Anat. Embryol. (Berl.) *149*, 87–112.

Diamond, J.S., and Jahr, C.E. (1997). Transporters buffer synapti-

cally released glutamate on a submillisecond time scale. J. Neurosci. *17*, 4672–4687.

Donevan, S.D., and Rogawski, M.A. (1995). Intracellular polyamines mediate inward rectification of Ca^{2+}-permeable α-amino-3-hydroxy-5-methyl-4-isoxazolepropionic acid receptors. Proc. Natl. Acad. Sci. USA *92*, 9298–9302.

Dzubay, J.A., and Jahr, C.E. (1999). The concentration of synaptically released glutamate outside of the climbing fiber-Purkinje cell synaptic cleft. J. Neurosci. *19*, 5265–5274.

Eccles, J.C., Llinas, R., and Sasaki, K. (1966). The inhibitory interneurones within the cerebellar cortex. Exp. Brain Res. *1*, 1–16.

Fortin, M., Marchand, R., and Parent, A. (1998). Calcium-binding proteins in primate cerebellum. Neurosci. Res. *30*, 155–168.

Gallo, V., Patneau, D.K., Mayer, M.L., and Vaccarino, F.M. (1994). Excitatory amino acid receptors in glial progenitor cells: molecular and functional properties. Glia *11*, 94–101.

Gallo, V., Zhou, J.M., McBain, C.J., Wright, P., Knutson, P.L., and Armstrong, R.C. (1996). Oligodendrocyte progenitor cell proliferation and lineage progression are regulated by glutamate receptor-mediated K+ channel block. J. Neurosci. *16*, 2659–2670.

Hall, A., Giese, N.A., and Richardson, W.D. (1996). Spinal cord oligodendrocytes develop from ventrally derived progenitor cells that express PDGF alpha-receptors. Development *122*, 4085–4094.

Hamori, J., and Szentagothai, J. (1980). Lack of evidence of synaptic contacts by climbing fibre collaterals to basket and stellate cells in developing rat cerebellar cortex. Brain Res. *186*, 454–457.

Hashimoto, K., and Kano, M. (1998). Presynaptic origin of paired-pulse depression at climbing fibre-Purkinje cell synapses in the rat cerebellum. J. Physiol. *506*, 391–405.

Huang, Y.H., and Bergles, D.E. (2004). Glutamate transporters bring competition to the synapse. Curr. Opin. Neurobiol. *14*, 346–352.

Huang, Y.H., Dykes-Hoberg, M., Tanaka, K., Rothstein, J.D., and Bergles, D.E. (2004). Climbing fiber activation of EAAT4 transporters and kainate receptors in cerebellar Purkinje cells. J. Neurosci. *24*, 103–111.

Huguenard, J.R. (1996). Low-threshold calcium currents in central nervous system neurons. Annu. Rev. Physiol. *58*, 329–348.

Ichikawa, R., Miyazaki, T., Kano, M., Hashikawa, T., Tatsumi, H., Sakimura, K., Mishina, M., Inoue, Y., and Watanabe, M. (2002). Distal extension of climbing fiber territory and multiple innervation caused by aberrant wiring to adjacent spiny branchlets in cerebellar Purkinje cells lacking glutamate receptor δ2. J. Neurosci. *22*, 8487–8503.

Iino, M., Goto, K., Kakegawa, W., Okado, H., Sudo, M., Ishiuchi, S., Miwa, A., Takayasu, Y., Saito, I., Tsuzuki, K., and Ozawa, S. (2001). Glia-synapse interaction through Ca2+-permeable AMPA receptors in Bergmann glia. Science *292*, 926–929.

Ito, M., and Kano, M. (1982). Long-lasting depression of parallel fiber-Purkinje cell transmission induced by conjunctive stimulation of parallel fibers and climbing fibers in the cerebellar cortex. Neurosci. Lett. *33*, 253–258.

Jorntell, H., and Ekerot, C.F. (2003). Receptive field plasticity profoundly alters the cutaneous parallel fiber synaptic input to cerebellar interneurons in vivo. J. Neurosci. *23*, 9620–9631.

Kano, M., Rexhausen, U., Dreessen, J., and Konnerth, A. (1992). Synaptic excitation produces a long-lasting rebound potentiation of inhibitory synaptic signals in cerebellar Purkinje cells. Nature *356*, 601–604.

Knutson, P., Ghiani, C.A., Zhou, J.M., Gallo, V., and McBain, C.J. (1997). K^+ channel expression and cell proliferation are regulated by intracellular sodium and membrane depolarization in oligodendrocyte progenitor cells. J. Neurosci. *17*, 2669–2682.

Kondo, T., and Raff, M. (2000). Oligodendrocyte precursor cells reprogrammed to become multipotential CNS stem cells. Science *289*, 1754–1757.

Koutmani, Y., Hurel, C., Patsavoudi, E., Hack, M., Gotz, M., Thomaidou, D., and Matsas, R. (2004). BM88 is an early marker of proliferating precursor cells that will differentiate into the neuronal lineage. Eur. J. Neurosci. *20*, 2509–2523.

Kreitzer, A.C., and Regehr, W.G. (2001). Retrograde inhibition of presynaptic calcium influx by endogenous cannabinoids at excitatory synapses onto Purkinje cells. Neuron *29*, 717–727.

Levine, J.M., and Card, J.P. (1987). Light and electron microscopic localization of a cell surface antigen (NG2) in the rat cerebellum: association with smooth protoplasmic astrocytes. J. Neurosci. *7*, 2711–2720.

LeVine, S.M., and Goldman, J.E. (1988). Spatial and temporal patterns of oligodendrocyte differentiation in rat cerebrum and cerebellum. J. Comp. Neurol. *277*, 441–455.

Levine, J.M., Reynolds, R., and Fawcett, J.W. (2001). The oligodendrocyte precursor cell in health and disease. Trends Neurosci. *24*, 39–47.

Levison, S.W., Chuang, C., Abramson, B.J., and Goldman, J.E. (1993). The migrational patterns and developmental fates of glial precursors in the rat subventricular zone are temporally regulated. Development *119*, 611–622.

Levison, S.W., Young, G.M., and Goldman, J.E. (1999). Cycling cells in the adult rat neocortex preferentially generate oligodendroglia. J. Neurosci. Res. *57*, 435–446.

Lin, S.C., and Bergles, D.E. (2002). Physiological characteristics of NG2-expressing glial cells. J. Neurocytol. *31*, 537–549.

Lin, S.C., and Bergles, D.E. (2004). Synaptic signaling between GABAergic interneurons and oligodendrocyte precursor cells in the hippocampus. Nat. Neurosci. *7*, 24–32.

Llano, I., Marty, A., Armstrong, C.M., and Konnerth, A. (1991). Synaptic- and agonist-induced excitatory currents of Purkinje cells in rat cerebellar slices. J. Physiol. *434*, 183–213.

Mallon, B.S., Shick, H.E., Kidd, G.J., and Macklin, W.B. (2002). Proteolipid promoter activity distinguishes two populations of NG2-positive cells throughout neonatal cortical development. J. Neurosci. *22*, 876–885.

Mariani, J., and Changeux, J.P. (1981). Ontogenesis of olivocerebellar relationships. II. Spontaneous activity of inferior olivary neurons and climbing fibermediated activity of cerebellar Purkinje cells in developing rats. J. Neurosci. *1*, 703–709.

Maricich, S.M., and Herrup, K. (1999). Pax-2 expression defines a subset of GABAergic interneurons and their precursors in the developing murine cerebellum. J. Neurobiol. *41*, 281–294.

Matsui, K., and Jahr, C.E. (2003). Ectopic release of synaptic vesicles. Neuron *40*, 1173–1183.

Matsui, K., and Jahr, C.E. (2004). Differential control of synaptic and ectopic vesicular release of glutamate. J. Neurosci. *24*, 8932–8939.

Medina, J.F., Nores, W.L., and Mauk, M.D. (2002). Inhibition of climbing fibres is a signal for the extinction of conditioned eyelid responses. Nature *416*, 330–333.

Muller, T., Moller, T., Neuhaus, J., and Kettenmann, H. (1996). Electrical coupling among Bergmann glial cells and its modulation by glutamate receptor activation. Glia *17*, 274–284.

Nishiyama, H., and Linden, D.J. (2004). Differential maturation of climbing fiber innervation in cerebellar vermis. J. Neurosci. *24*, 3926–3932.

Nishiyama, A., Lin, X.H., Giese, N., Heldin, C.H., and Stallcup, W.B. (1996). Co-localization of NG2 proteoglycan and PDGF alpha-receptor on O2A progenitor cells in the developing rat brain. J. Neurosci. Res. *43*, 299–314.

Nishiyama, A., Chang, A., and Trapp, B.D. (1999). NG2+ glial cells: a novel glial cell population in the adult brain. J. Neuropathol. Exp. Neurol. *58*, 1113–1124.

Nishiyama, A., Watanabe, M., Yang, Z., and Bu, J. (2002). Identity, distribution, and development of polydendrocytes: NG2-expressing glial cells. J. Neurocytol. *31*, 437–455.

Ohyama, T., Nores, W.L., Murphy, M., and Mauk, M.D. (2003). What the cerebellum computes. Trends Neurosci. *26*, 222–227.

Oliet, S.H., Malenka, R.C., and Nicoll, R.A. (1996). Bidirectional control of quantal size by synaptic activity in the hippocampus. Science *271*, 1294–1297.

Ong, W.Y., and Levine, J.M. (1999). A light and electron microscopic

study of NG2 chondroitin sulfate proteoglycan-positive oligodendrocyte precursor cells in the normal and kainate-lesioned rat hippocampus. Neuroscience *92*, 83–95.

Otis, T.S., Kavanaugh, M.P., and Jahr, C.E. (1997). Postsynaptic glutamate transport at the climbing fiber-Purkinje cell synapse. Science *277*, 1515–1518.

Overstreet, L.S., Hentges, S.T., Bumaschny, V.F., de Souza, F.S., Smart, J.L., Santangelo, A.M., Low, M.J., Westbrook, G.L., and Rubinstein, M. (2004). A transgenic marker for newly born granule cells in dentate gyrus. J. Neurosci. *24*, 3251–3259.

Palay, S.L., and Chan-Palay, V. (1974). Cerebellar Cortex: Cytology and Organization (Berlin: Springer).

Patneau, D.K., Vyklicky, L., Jr., and Mayer, M.L. (1993). Hippocampal neurons exhibit cyclothiazide-sensitive rapidly desensitizing responses to kainate. J. Neurosci. *13*, 3496–3509.

Patneau, D.K., Wright, P.W., Winters, C., Mayer, M.L., and Gallo, V. (1994). Glial cells of the oligodendrocyte lineage express both kainate- and AMPA-preferring subtypes of glutamate receptor. Neuron *12*, 357–371.

Pende, M., Holtzclaw, L.A., Curtis, J.L., Russell, J.T., and Gallo, V. (1994). Glutamate regulates intracellular calcium and gene expression in oligodendrocyte progenitors through the activation of DL-α-amino-3-hydroxy-5-methyl-4-isoxazolepropionic acid receptors. Proc. Natl. Acad. Sci. USA *91*, 3215–3219.

Peters, A. (2004). A fourth type of neuroglial cell in the adult central nervous system. J. Neurocytol. *33*, 345–357.

Peters, A., Palay, S.L., and Webster, H. (1991). The Fine Structure of the Nervous System: Neurons and Their Supporting Cells, Third Edition (New York: Oxford University Press).

Rammes, G., Parsons, C., Muller, W., and Swandulla, D. (1994). Modulation of fast excitatory synaptic transmission by cyclothiazide and GYKI 52466 in the rat hippocampus. Neurosci. Lett. *175*, 21–24.

Regehr, W.G., and Mintz, I.M. (1994). Participation of multiple calcium channel types in transmission at single climbing fiber to Purkinje cell synapses. Neuron *12*, 605–613.

Rossi, F., Borsello, T., Vaudano, E., and Strata, P. (1993). Regressive modifications of climbing fibres following Purkinje cell degeneration in the cerebellar cortex of the adult rat. Neuroscience *53*, 759–778.

Shihabuddin, L.S., Horner, P.J., Ray, J., and Gage, F.H. (2000). Adult spinal cord stem cells generate neurons after transplantation in the adult dentate gyrus. J. Neurosci. *20*, 8727–8735.

Silver, R.A., Momiyama, A., and Cull-Candy, S.G. (1998). Locus of frequency-dependent depression identified with multiple-probability fluctuation analysis at rat climbing fibre-Purkinje cell synapses. J. Physiol. *510*, 881–902.

Spacek, J. (1985). Three-dimensional analysis of dendritic spines. III. Glial sheath. Anat. Embryol. (Berl.) *171*, 245–252.

Sugihara, I., Wu, H., and Shinoda, Y. (1999). Morphology of single olivocerebellar axons labeled with biotinylated dextran amine in the rat. J. Comp. Neurol. *414*, 131–148.

Tillet, E., Ruggiero, F., Nishiyama, A., and Stallcup, W.B. (1997). The membrane-spanning proteoglycan NG2 binds to collagens V and VI through the central nonglobular domain of its core protein. J. Biol. Chem. *272*, 10769–10776.

Wadiche, J.I., and Jahr, C.E. (2001). Multivesicular release at climbing fiber-Purkinje cell synapses. Neuron *32*, 301–313.

Wang, D.D., Krueger, D.D., and Bordey, A. (2003). GABA depolarizes neuronal progenitors of the postnatal subventricular zone via $GABA_A$ receptor activation. J. Physiol. *550*, 785–800.

Weyer, A., and Schilling, K. (2003). Developmental and cell type-specific expression of the neuronal marker NeuN in the murine cerebellum. J. Neurosci. Res. *73*, 400–409.

Windrem, M.S., Nunes, M.C., Rashbaum, W.K., Schwartz, T.H., Goodman, R.A., McKhann, G., Roy, N.S., and Goldman, S.A. (2004). Fetal and adult human oligodendrocyte progenitor cell isolates myelinate the congenitally dysmyelinated brain. Nat. Med. *10*, 93–97.

Wyllie, D.J., Mathie, A., Symonds, C.J., and Cull-Candy, S.G. (1991). Activation of glutamate receptors and glutamate uptake in identified macroglial cells in rat cerebellar cultures. J. Physiol. *432*, 235–258.

Xu-Friedman, M.A., and Regehr, W.G. (2003). Ultrastructural contributions to desensitization at cerebellar mossy fiber to granule cell synapses. J. Neurosci. *23*, 2182–2192.

Ye, P., Bagnell, R., and D'Ercole, A.J. (2003). Mouse NG2+ oligodendrocyte precursors express mRNA for proteolipid protein but not its DM-20 variant: a study of laser microdissection-captured NG2+ cells. J. Neurosci. *23*, 4401–4405.

Yuan, X., Eisen, A.M., McBain, C.J., and Gallo, V. (1998). A role for glutamate and its receptors in the regulation of oligodendrocyte development in cerebellar tissue slices. Development *125*, 2901–2914.

Zenisek, D., Steyer, J.A., and Almers, W. (2000). Transport, capture and exocytosis of single synaptic vesicles at active zones. Nature *406*, 849–854.

Zhang, L., and Goldman, J.E. (1996). Developmental fates and migratory pathways of dividing progenitors in the postnatal rat cerebellum. J. Comp. Neurol. *370*, 536–550.